Application of ac tomography to crack identification

H. Saguy and D. Rittel[a)]
Faculty of Mechanical Engineering, Technion, 32000 Haifa, Israel

(Received 22 June 2007; accepted 1 August 2007; published online 24 August 2007)

The depth of penetration of alternating currents in conductors depends on their frequency and material properties. A tomographiclike technique was proposed, in which the frequency is systematically varied to detect and size flaws (emerging and hidden) in electrical conductors, based on an analysis of the skin effect [Saguy and Rittel, Appl. Phys. Lett. **89**, 094107 (2006); **87**, 084103 (2005)]. Initial results were reported for notched specimens [Saguy and Rittel, NDT & E Int. **40**, 505 (2007)] This letter presents experimental results on the detection of actual sharp fatigue cracks, differing from notches in terms of sharpness and partial conduction through the crack flanks. The results show that hidden cracks with arbitrary crack-front shape can be accurately identified.
 [DOI: 10.1063/1.2775046]

The detection and evaluation of flaws (surface and internal) in metals is of prime importance during the manufacturing and service life of a structural component. Among the various non destructive techniques, the alternating current potential drop (acPD) is used to evaluate the depth of surface breaking cracks. The technique is based on the skin effect phenomenon. Namely, when an alternate current (ac) flows in a conductor, it concentrates in a thin surface skin. The skin thickness δ depends on the metal properties and the current frequency f and is given by

$$\delta = \frac{1}{(\pi \mu_r \mu_0 \sigma f)^{1/2}}, \tag{1}$$

where μ_r is the relative magnetic permeability, μ_0 is the magnetic permeability of free space, and σ is the electrical conductance.[1–3]

Practically, the crack depth d is evaluated based on measuring voltage drops V_2 and V_1 across the crack and far from it, respectively. The skin thickness (δ), part thickness (t) and crack depth (d) all define thin or thick skin conditions.[4–6] For a thin skin condition, the crack depth can be directly calculated from Eq. (2).[7–9]

$$d = \frac{\Delta}{2}\left(\frac{V_2}{V_1} - 1\right). \tag{2}$$

Equation (2) and the corresponding thin skin condition were, until recently, the basic requirements for accurate crack assessments. Saguy and Rittel[10] lifted this restriction by proposing solution that bridges thin and thick skin conditions in a seamless manner, as expressed by Eq. (3),

$$\frac{V_2}{V_1} = \frac{\Delta + 2d - f_1(\Delta, \delta) - f_2(d, \delta)}{\Delta}. \tag{3}$$

The reader is referred to Ref. 10 for additional details on the expressions f_1 and f_2.

A straightforward application of this result is that the skin thickness [Eq. (1)] can be systematically varied (modulated) in a tomographiclike fashion. The flawed part can be scanned from high (thin skin) to low (thick skin) frequency in order to reveal hidden flaws and their depth. A basic relation between the skin thickness δ and the uncracked thickness, $t-d$ was identified,[11]

$$\frac{\delta}{(t-d)} = 0.5. \tag{4}$$

This relation was applied experimentally to assess the depth of a straight-fronted sharp notch in plate specimens made of various conducting metallic alloys.[12]

However, as sharp as it can be, a notch differs from a sharp crack in terms of its small tip radius of curvature and the fact that some contact may exist between the crack flanks, due to natural asperities that do not otherwise exist for a straight notch. A second issue relates to the fact that actual cracks are very seldom straight fronted, so that $d=d(y)$ in Eq. (3), and the problem is no longer one dimensional. Proper assessment of the curvature of the crack front is of prime importance for fracture mechanics calculations.

These two issues are the central theme of this letter, namely, the application of electrical ac tomography to actual sharp cracks with arbitrary crack-front curvature. To address these, an experimental methodology, extending the previous one, is applied to different materials and experiments. The main outcome of this work is that arbitrary crack-front geometries can accurately be determined for sharp fatigue cracks, whether hidden of surface breaking or not. These results generalize the proposed method and its applications to include actual situations.

In a typical experiment, the uniform crack-front depth is assessed from a couple of measurements, V_2 and V_1. To characterize a curved crack front, several pairs of measurements must be carried out along the crack line, namely, $V_2(y)$ and $V_1(y)$. The shape of the crack front, $d(y)$, is obtained from Eq. (2), or, more generally, from Eq. (3). Two possibilities were considered in this work: surface breakings cracks whose depth is to be determined and bottom cracks, also surface breaking, but invisible since located on the hidden side of the specimen. In all the cases, the skin depth is controlled by the frequency of the ac current. For a surface breaking crack, Eqs. (1)–(3) are used, whereas for a bottom (hidden) crack, Eqs. (1) and (4) are used. Figure 1 illustrates schematically a bottom crack experiment, for which pairs of $V_2(y)$ and $V_1(y)$ are measured.

[a)]Author to whom correspondence should be addressed; electronic mail merittel@technion.ac.il

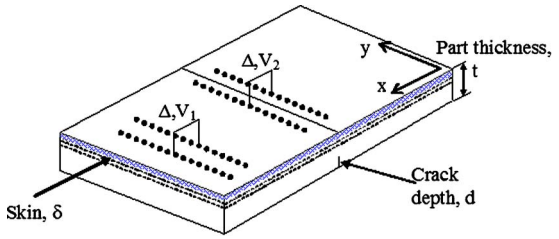

FIG. 1. Schematic description of the tomography principle for a bottom crack configuration. Pairs of measurements $V_2(y)$ and $V_1(y)$ are taken along the crack line (y).

Fatigue cracks were grown by applying cyclic three point bending to notched rectangular beam specimens. The beams were made of mild steel and of stainless steel to vary the skin condition. The cracks were located in the center of the blocks, where the electric field is constant. The materials, their magnetic and electrical properties, and specimens' dimensions are summarized in Table I. The actual dimensions of the crack were unknown throughout the tests. Upon completion, the specimens were broken open to reveal the actual fatigue crack shape and dimensions.

The experimental system consisted of an ac signal generator, power amplifier (operated as a constant current operational amplifier at frequencies of 5–20 KHz), probes (homemade, consisting of two electrodes), voltage amplifier, and a digital oscilloscope. The system was set to the following specifications: generated current $I=0.5-2$ A, frequency of 5–20 kHz, and distance between the probes (fixed) of $\Delta=10$ mm. The electrodes are sharp needles, with a typical tip contact area of about 0.1 mm^2. The probe was moved ±12.5 mm from the center line along the y axis.

The first set of measurements was carried out on the steel specimens with the fatigue surface crack (set 1, Table I).

A comparison between the thin skin approximation [Eq. (2)], proposed equation [Eq. (3)] and the actual crack depth (measured after breaking) is given in Fig. 2(a).

At each measured point along the y axis, three sets of measurements (both V_2 and V_1) were taken over a range of frequencies (5–20 kHz). The estimated crack depth was calculated by Eqs. (2) and (3) for each frequency. Figure 2(a) presents the average values of the estimated crack depth. The error bars present the deviations for different frequencies and for the three measurements. Figure 2(b) shows a picture of the specimen (2) after breaking it open.

Since all the measurements were taken at thin skin conditions (for steel, the skin thickness is about 0.2–0.1 mm at frequencies of 5–20 kHz), the thin skin approximation [Eq. (2)] and the proposed equation [Eq. (3)] give similar values for the crack depth. The maximum error between the evaluated and actual crack depths is less then 10%.

TABLE I. Materials, properties, and dimensions of the specimens.

Set	Material and Properties	Length (mm)	Width (mm)	Thickness (mm)
1	AISI 1020—steel, $\mu_0=500$, $\sigma=5.8$ MS/m	200	45	25
2	SAE 304 L—stainless steel, $\mu_0=1$, $\sigma=1.36$ MS/m	200	45	20

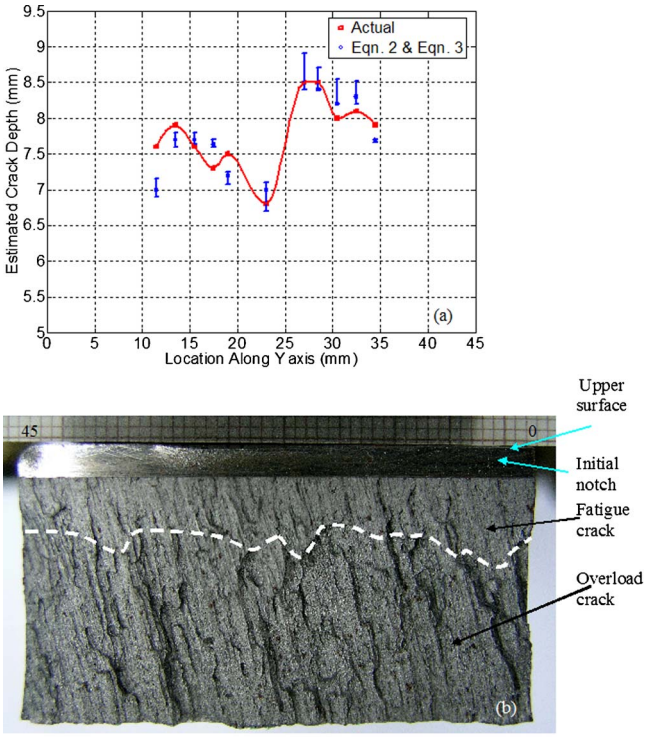

FIG. 2. (a) Crack-front shape, as determined from Eqs. (2) and (3) for a surface breaking crack in carbon steel, in thin skin configuration, and the actual fatigue crack. Note the excellent agreement between the actual crack-front shape and the experimental predictions. (b) Specimen (2) [of (a)] after being open in the laboratory.

The second set of measurements was carried out on stainless steel specimens in the surface breaking and the bottom crack configurations, the latter being obtained by flipping the specimen.

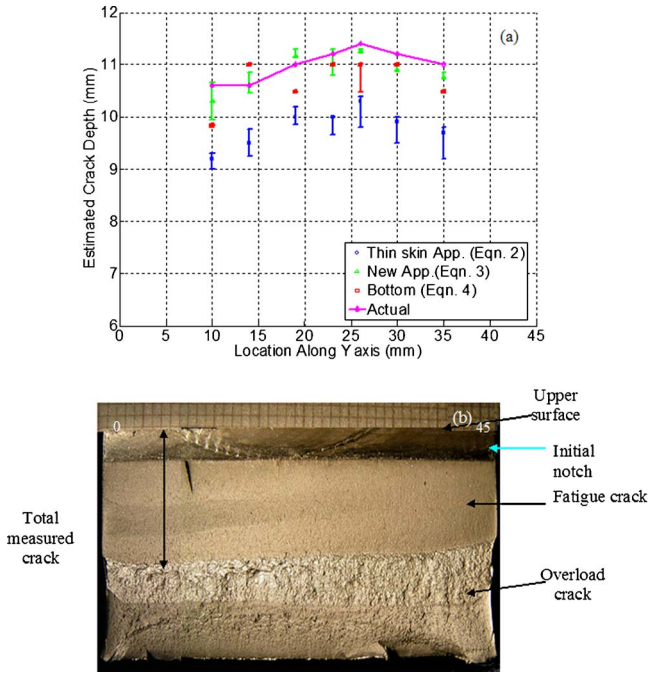

FIG. 3. (a) Crack-front profile, as determined from surface, bottom, and actual measurements. Surface data are processed assuming a thin skin and the proposed approximation. Note the excellent agreement between the actual crack-front profile and its estimates using bottom measurements and the proposed approximation for surface measurements. (b) Specimen (4) [of (a)] after being open in the laboratory.

Figure 3(a) shows a comparison between the thin skin approximation [Eq. (2)], the proposed equation [Eq. (3)], bottom crack measurements obtained after flipping the specimen [Eq. (4)], and the actual crack depth (measured after breaking). Figure 3(b) shows a picture of the specimen (4) after breaking it open.

Since thick skin conditions prevail here (for stainless steel the skin thickness is about 6–3 mm at frequency of 5–20 kHz), the results show that the thin skin approximation [Eq. (2)] yields a significant error (underestimation) of the crack-front shape estimation. By contrast, Eqs. (3) and (4) provides a similar estimation of the crack front shape, which also matches quite accurately the actual measurements. The maximum error for the evaluated crack depth based on thin skin approximation is 13%, which drops to 3% using Eq. (3) and to 7% using Eq. (4).

The novelty of this work lies in the testing of sharp fatigue (actual) cracks that are sharper than any machined notch, and for which the crack flanks are in partial contact, thus inducing some noise in the measurements. The present results show that actual sharp fatigue cracks can be accurately sized by ACPD measurements [Eqs. (3) and (4)], including a faithful reconstruction of a curved crack front of any shape. This last point represents a significant progress upon other methods which may be significantly more complex (including possibly an inverse problem approach) than the method developed and used here. A potential future application of this work is the real-time monitoring of the crack-front evolution of dynamically propagating cracks.

[1]N. Bowler, J. Phys. D **39**, 584 (2006).
[2]N. Bowler, IEEE Trans. Magn. **41**, 2102 (2005).
[3]W. C. Johnson, *Transmission Lines and Networks* (McGraw-Hill, New York, 1950), pp. 58–80.
[4]R. Collins, W. D. Dover, and D. H. Michael, in *Nondestructive Testing* edited by R. S. Sharpe (Academic, New York, 1985), Chap. 5, p. 211.
[5]M. C. Lugg, NDT Int. **22**, 149 (1989).
[6]D. Mirshekar-Syahkal, R. Collins, and D. H. Michael, J. Nondestruct. Eval. **3**, 65 (1982).
[7]M. C. Lugg, NDT Int. **21**, 153 (1988).
[8]W. D. Dover, F. D. Charlesworth, K. A. Taylor, R. Collins, and D. H. Michael, in *The Measurement of Crack Length and Shape During Fracture and Fatigue*, edited by C. J. Beevers (Cradley Heath, England, 1980), p. 222.
[9]W. D. Dover and C. C. Monahan, Fatigue Fract. Eng. Mater. Struct. **17**, 1485 (1994).
[10]H. Saguy and D. Rittel, Appl. Phys. Lett. **87**, 084103 (2005).
[11]H. Saguy and D. Rittel, Appl. Phys. Lett. **89**, 094102 (2006).
[12]H. Saguy and D. Rittel, NDT & E Int. **40**, 505 (2007).